14 International Journal of Air-Conditioning and Refrigeration Volume 8 May (2000) / pp. 14~28

Frequency Response Characteristics of Air-Cooled Condenser in Case of Inputting Various Disturbances

Jae-Dol Kim*, Hoo-Kyu Oh** and Jung-In Yoon**

Key words : Dynamic Characteristics, Refrigeration Systems, Air Conditioning Systems, Transfer Function, Frequency Response, Condenser

Abstract

The frequency response characteristics of a condenser were numerically studied for the control of refrigeration and air conditioning systems. The important parameters, such as the refrigerant flow rate, refrigerant temperature, air velocity, and air temperature at the condenser inlet, were analyzed. Superheated vapor, two phase, and subcooled liquid domain in condenser can be described by using the energy balance equation and the mass balance equation in refrigerant and tube wall, the basic equation for describing the dynamic characteristics of condenser can be derived. The transfer function for describing dynamic response of the condenser to disturbances can be obtained from using linearizations and Laplace transformations of the equation. From this transfer function, analytical investigation which affects the frequency responses of condenser has been made. Block diagrams were made based on the analytic transfer function; dynamic responses were evaluated in Bode diagrams on the frequency response.

Through this study, it became possible that the information about the dynamic characteristics of air-cooled condenser is offered. The results may be used for determining the optimum design parameters in actual components and entire systems. Also, the mathematical models, frequency response may be used to help understanding, evaluate optimum design parameters, design control systems and determine on setting the best controller for the refrigeration and air-conditioning systems.

* Member of SAREK, Dept. of Architectural Equipment, Tong Myong College, Pusan, 608-740, Korea

** Member of SAREK, Dept. of Refrigeration Engineering and Air Conditioning, Pukyong National University, Pusan, 608-737, Korea

Nomenclature

A : Area, [㎡]
C_m : Heat capacity, [J/kgK]
C_p : Specific heat, [J/kgK]
H : Enthalpy, [J/kg]
K : Heat transfer rate of unit length, [W/mK]
L : Length, [m]
l : Dimensionless length, [-]
M : Mass flow rate, [kg/s]
Q : Heat transfer rate, [W]
t : Time, [s]
v : Velocity, [m/s]
α : Heat transfer coefficient, [W/㎡K]
Θ : Temperature, [K]
ρ : Density, [kg/㎥]

Subscripts

0 : Steady state
1~9 : boundary
a : Air
d : Discharge
g : Saturated vapor
I : Interface
id : Internal circumference
in : Inlet
L : Condensation ending region
m : Tube wall
o : External
od : External circumference
out : Outlet
r : Refrigerant
s : Superheated vapor
shm : Average of internal division
sT : Condensation starting region
T : Boundary 4~6
Δ : Infinitesimal change
— : Average

1. Introduction

Recently the high efficiency of a system and the comfort of people using the system under various conditions have been required for the design of refrigeration and air-conditioning systems. But optimum control and sufficient cycle efficiency have not been obtained easily in the view of total operation. To explain this, the dynamic characteristic analysis is coming to the front of seriously essential subject. But the refrigeration and air-conditioning system is combined in several composition element, especially the evaporator or condenser as a heat exchanger go with heat and mass transfer according to phase-change so that characteristic analysis is very difficult.[1~4] And most refrigeration and air-conditioning systems operate under various conditions, pure steady-state does not exist. Especially if the capacity controllers fit to a system, investigations should not be limited to only the steady-state analysis but include indeed even the unsteady or dynamic-state analysis.[5] Even though a few experimental and theoretical studies have been done until now, the analysis of this part has not offered any clear answer.

Accordingly, the purpose of this study is to give an analysis of the dynamic characteristics of the air-cooled condenser in order to analyze the dynamic characteristics of entire refrigeration and air-conditioning systems.[6~7] The dynamic characteristic was performed with obtaining data which the radiant heat quantity of each region and the average heat transfer coefficient, the refrigerant and tube wall temperature distribution, pressure drop through advanced static characteristic analysis.[8~9]

The dynamic model was divided into five regions : the superheated vapor region, the

condensation starting region, two-phase condensation region, condensation ending region, and the subcooled liquid region. Furthermore transfer functions were derived from basic equations. Thus, the dynamic characteristics of an air-cooled condenser were analyzed theoretically by the frequency response method. Moreover, these analytic results offered not only the response of the condenser caused by the various disturbance inputs but also the cause of the response occurrence, which made it possible to obviously specify the effect of condenser design parameters qualitatively and quantitatively.[10~12]

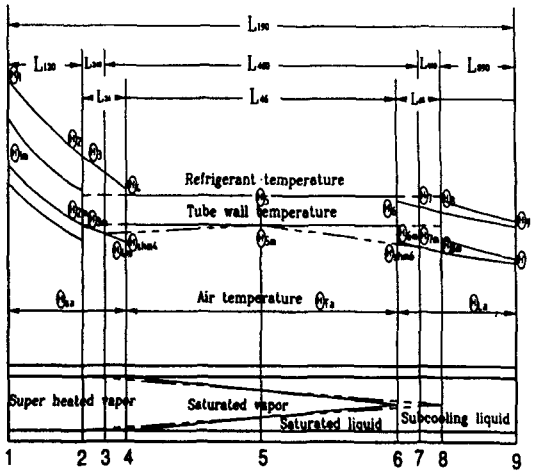

Fig. 1 Model of dynamic characteristics of air-cooled condenser.

2. Analysis Model

The dynamic model, as in the static model, was formed by using a plate-fin coil type air-cooled condenser. According to the model of the refrigerant and tube-wall temperature distribution in the static characteristics analysis, the refrigerant in the actual condenser is flowed in as a superheated vapor and is flowed out as a subcooled liquid. It always has temperature distribution throughout this process, and the heat transfer coefficient on the refrigerant side changes depending on the inlet point. For these reasons, linearization of basic equations is mathematically complicated and it is difficult to derive form of the transfer functions based on analysis of the dynamic characteristics.[13~15]

Figure 1 shows the model of this study. The analysis was accomplished with the model. In this model, overall region was divided into 5 subregions consisting of the superheated-vapor region(boundary 1 to 2), the condensation starting region(boundary 2 to 4), the two-phase condensing region(boundary 4 to 6), the condensation ending region(boundary region 6 to 8), and the subcooled-liquid region(boundary 8 to 9). In the model, the heat transfer rate should be consistent in both the static and dynamic analysis. Thus, the heat transfer coefficient was obtained in each region and the average heat transfer rate was calculated from these results.

2.1 Assumptions

The assumptions of the mathematical model are as follows:

(1) The average heat transfer coefficient on the air side is assumed to be a convection heat transfer coefficient except the effect of humidity.

(2) The two-phase refrigerant has linear quality distribution and the state of refrigerant is saturation.

(3) Pressure drop was considered only in the two-phase region. Because the two-phase condensing region has a larger pressure drop in comparing with any other region in the analysis of static characteristics.

(4) The changes of condensing pressure and temperature in the two-phase region are assumed to be equal to an infinitesimal change of refrigerant flow rate.

2.2 Basic equations

The basic equations of the dynamic analysis are the continuity equation, energy balance equation, and heat transfer equation based on the above assumptions.

The superheated-vapor region takes the control volume into consideration between boun daries 1 and 2. In this region, the continuity equation and the energy balance equation of the refrigerant and tube wall are given by:

$$M_1 - M_2 \fallingdotseq 0 \tag{1}$$

$$A\rho_{\overline{12}} c_{p\overline{12}} \frac{\partial \Theta_2}{\partial t} = -\frac{M_1 c_{p\overline{12}}}{L_{12}} \frac{\partial \Theta_2}{\partial l_2} - \alpha_s A_i (\Theta_2 - \Theta_{2m}) \tag{2}$$

$$C_m \frac{\partial \Theta_{2m}}{\partial t} = \alpha_s A_i (\Theta_2 - \Theta_{2m}) - \alpha_a A_o (\Theta_{2m} - \Theta_a) \tag{3}$$

The condensation starting region is short and the control volume is set between boundaries 2 and 4. Boundary 3 is defined in the middle plane of boundaries 2 to 4. Also, the refrigerant properties and the temperature distribution of the tube wall are assumed to be linear. The continuity equation, energy balance equation of the refrigerant and tube wall are given by:

$$M_2 - M_4 = A\left[\frac{d}{dt}(\rho_3 L_{24}) - \rho_4 \frac{dL_{24}}{dt}\right] \tag{4}$$

$$M_2 H_2 - M_4 H_4 - Q_{24} = A\left[\frac{d}{dt}(\rho_3 H_3 L_{24}) - \rho_4 H_4 \frac{dL_{24}}{dt}\right] \tag{5}$$

$$C_m L_{24} \frac{d\Theta_{3m}}{dt} = \alpha_{sT} A_i L_{24} (\Theta_3 - \Theta_{3m}) - \alpha_a A_o L_{24} (\Theta_{3m} - \Theta_a) \tag{6}$$

where Q_{24} of Eq. (5) can be written as:

$$Q_{24} = \alpha_{sT} A_i L_{24} (\Theta_3 - \Theta_{3m}) + C_m (\Theta_{3m} - \Theta_{shm4}) \frac{dL_{24}}{dt} \tag{7}$$

The two-phase condensing region takes the control volume into consideration between boundaries 4 and 6. Boundary 5 is defined in the middle point of boundaries 4 to 6. Also, the refrigerant properties and the temperature distribution of the tube wall are assumed to be linear. Each equation of this region is given by:

$$M_4 - M_6 = A\left[\frac{d}{dt}(\overline{\rho_5} L_{46}) - \rho_4 \frac{dL_{24}}{dt} + \rho_6 \frac{dL_{68}}{dt}\right] \tag{8}$$

$$M_4 H_4 - M_6 H_6 - Q_{46} = A\left[\frac{d}{dt}(\overline{\rho_5 H_5} L_{46}) + \rho_4 H_4 \frac{dL_{24}}{dt} + \rho_6 H_6 \frac{dL_{68}}{dt}\right] \tag{9}$$

$$C_m L_{46} \frac{d\Theta_{5m}}{dt} = \alpha_T A_i L_{46} (\Theta_5 - \Theta_{5m}) - \alpha_a A_o L_{46} (\Theta_{5m} - \Theta_a) \tag{10}$$

where Q_{46} of Eq. (9) is given by:

$$Q_{46} = \alpha_T A_i L_{46} (\Theta_5 - \Theta_{3m}) + C_m (\Theta_{shm4} - \Theta_{5m}) \frac{dL_{24}}{dt} - C_m (\Theta_{5m} - \Theta_{shm6}) \frac{dL_{68}}{dt} \tag{11}$$

The condensation ending region is short and the control volume is taken into consideration at boundary 6 to 8. Boundary 7 is defined in the middle point of boundaries 6 to 8. Also, the refrigerant properties and the temperature distribution of the tube wall are assumed to be linear. Under these assumptions, each equation of this region is given by:

$$M_6 - M_8 = A\left[\frac{d}{dt}(\rho_7 L_{68}) - \rho_6 \frac{dL_{68}}{dt}\right] \tag{12}$$

$$M_6 H_6 - M_8 H_8 - Q_{68}$$

$$= A\left[\frac{d}{dt}(\rho_7 H_7 L_{68}) - \rho_6 H_6 \frac{dL_{68}}{dt}\right] \quad (13)$$

$$C_m L_{68}\frac{d\Theta_{7m}}{dt} = \alpha_L A_i L_{68}(\Theta_7 - \Theta_{7m}) - \alpha_a A_o L_{68}(\Theta_{7m} - \Theta_a) \quad (14)$$

where Q_{68} of Eq. (13) is equal to Eq. (15).

$$Q_{68} = \alpha_L A_i L_{68}(\Theta_7 - \Theta_{7m}) - C_m(\Theta_{shm6} - \Theta_{7m})\frac{dL_{68}}{dt} \quad (15)$$

The subcooled-liquid region takes the control volume into consideration between boundaries 8 and 9. Each equation of this region can be written as follows:

$$M_8 - M_9 \fallingdotseq 0 \quad (16)$$

$$A\rho_{\overline{89}} c_{p\overline{89}}\frac{\partial \Theta_9}{\partial t} = -\frac{M_8 c_{p\overline{89}}}{L_{89}}\frac{\partial \Theta_2}{\partial l_9} - \alpha_L A_i(\Theta_9 - \Theta_{9m}) \quad (17)$$

$$C_m\frac{d\Theta_{9m}}{dt} = \alpha_L A_i L_{68}(\Theta_9 - \Theta_{9m}) - \alpha_a A_o(\Theta_{9m} - \Theta_a) \quad (18)$$

2.3 The combination and linearization of basic equations

From the combination of the energy balance equation, the continuity equation and the heat transfer equation of the refrigerant and tube wall each change in quantities($Y = Y_0 + y$) can be written as sums of the equilibrium state quantity Y_0 and perturbation quantity y. The energy equations of the refrigerant and tube wall in the superheated-vapor region are linearized to obtain the response of refrigerant temperature θ_2 in boundary 2 with the refrigerant inlet temperature θ_1, the flowed in air temperature θ_a and air velocity v_a . The linearized energy balance equations of the refrigerant and tube wall are given by:

$$\frac{\partial \theta_2}{\partial l_2} + \frac{A\rho_{\overline{120}} L_{120}}{M_{90}}\frac{\partial \theta_2}{\partial t} + \frac{\alpha_{s0} A_i L_{120}}{M_{90} c_{p\overline{120}}}\theta_2 = \frac{\alpha_{s0} A_i L_{120}}{M_{90} c_{p\overline{120}}}\theta_{2m} \quad (19)$$

$$\frac{C_m}{\alpha_{s0} A_i + \alpha_{a0} A_o}\frac{\partial \theta_{2m}}{\partial t} + \theta_{2m} = \frac{\alpha_{s0} A_i}{\alpha_{s0} A_i + \alpha_{a0} A_o}\theta_2 + \frac{\alpha_{s0} A_o}{\alpha_{s0} A_i + \alpha_{a0} A_o}\theta_a - \frac{A_o(\Theta_{2m0} - \Theta_{a0})}{\alpha_{s0} A_i + \alpha_{a0} A_o}\Delta\alpha_a \quad (20)$$

The linearized energy balance equations of the refrigerant and tube wall according to the changes of the refrigerant flow rate m_1 are given by:

$$\frac{\partial \theta_2}{\partial l_2} + \overline{\tau}_{a10}\frac{\partial \theta_2}{\partial t} + \frac{\alpha_{10}}{\gamma_{a10}}(\theta_2 - \theta_{2m}) - \alpha_{10}\left(\frac{\Delta\alpha_1}{\alpha_{10}} - \frac{\Delta\gamma_{a1}}{\gamma_{a10}}\right)(\Theta_{10} - \Theta_{a0})\, e^{-\alpha_{10} l_2} \quad (21)$$

$$\theta_{2m} + \overline{\tau}_{w10}\frac{\partial \theta_{2m}}{\partial t} = \gamma_{b10}\theta_2 - \Delta\gamma_{a1}(\Theta_{10} - \Theta_{a0})\, e^{-\alpha_{10} l_2} \quad (22)$$

Also, the same method for the superheated-vapor region, the linearized equations of the condensation starting region when the refrigerant flow rate changes are given by:

$$\begin{aligned} &m_4(H_{20} - H_{40}) = -M_{90} c_{p24}(\theta_2 - \theta_5) \\ &+ \alpha_{s0} A_i L_{240}(\theta_3 - \theta_{3m}) + \alpha_{s0} A_i(\Theta_{30} - \Theta_{3m0})\,\ell_{24} \\ &- AL_{240}(H_{20} - H_{30})\left[\left\{\frac{\partial \rho_3}{\partial P_d}\right\}_{\Theta_{30}}\left\{\frac{\partial P_d}{\partial T_4}\right\} + \left\{\frac{\partial \rho_3}{\partial T_3}\right\}_{P_d}\right]\frac{d\theta_3}{dt} + \frac{1}{2}A\rho_{30} L_{240} c_{p24}\frac{d\theta_2}{dt} \\ &+ \frac{1}{2}A\rho_{30} L_{240} c_{p24}\frac{d\theta_5}{dt} - [A\{\rho_{30}(H_{20} - H_{30}) - \rho_{40}(H_{20} - H_{40})\} - C_m(\Theta_{3m0} - \Theta_{shm40})]\frac{d\ell_{24}}{dt} \end{aligned} \quad (23)$$

$$m_4 = m_9 - A(\rho_{70} - \overline{\rho}_{50})\frac{dl_{46}}{dt} - A(\rho_{70} - \rho_{40})\frac{dl_{24}}{dt} + AL_{460}\left(\frac{\partial \overline{\rho}_5}{\partial \theta_5}\right)_0 \frac{d\theta_5}{dt} \quad (24)$$

The linearized equations of the two-phase region are given by:

$$m_6(H_{40} - H_{60}) = -M_{90}\left[\left(\frac{\partial H_4}{\partial \Theta_4}\right)_0 - \left(\frac{\partial H_6}{\partial \Theta_6}\right)_0\right]\theta_5 + \alpha_{T0}A_iL_{460}(\theta_5 - \theta_{5m}) + \alpha_{T0}A_i(\Theta_{50} - \Theta_{5m0})l_{46} + [A\rho_{60}(H_{40} - H_{60}) + C_m(\Theta_{shm40} - \Theta_{shm60})]\frac{dl_{24}}{dt} + [A\{\rho_{60}(H_{40} - H_{60}) - (\rho_{50}H_{40} - \overline{\rho_{50}H_{50}})\} + C_m(\Theta_{5m0} - \Theta_{shm60})]\frac{dl_{46}}{dt} + AL_{460}\left[\left(\frac{\partial \overline{\rho_5 H_5}}{\partial \Theta_5}\right)_0 - H_{40}\left(\frac{\partial \overline{\rho_5}}{\partial \Theta_5}\right)_0\right]\frac{d\theta_5}{dt} \quad (25)$$

$$m_6 = m_9 - A(\rho_{70} - \rho_{60})\frac{dl_{24}}{dt} - A(\rho_{70} - \rho_{60})\frac{dl_{46}}{dt} \quad (26)$$

The linearized equations of the condensation ending region are given by:

$$m_9(H_{60} - H_{80}) = -M_{90}c_{p68}(\theta_5 + \theta_8) + \alpha_{L0}A_iL_{680}(\theta_7 + \theta_{7m}) - \alpha_{L0}A_i(\Theta_{70} - \Theta_{7m0}) + (l_{24} + l_{46}) + A\rho_{70}L_{680}\frac{c_{p68}}{2}\frac{d\theta_5}{dt} + A\rho_{70}L_{680}\frac{c_{p68}}{2}\frac{d\theta_8}{dt} + [A\rho_{70}(H_{60} - H_{70}) + C_m(\Theta_{shm60} - \Theta_{7m0})]\left(\frac{dl_{24}}{dt} + \frac{dl_{46}}{dt}\right) \quad (27)$$

$$C_m\frac{d\theta_{7m}}{dt} = \alpha_{L0}A_i\theta_7 - (\alpha_{L0}A_i + \alpha_{a0}A_o)\theta_{7m} \quad (28)$$

where

$$\gamma_{a1} = \frac{\alpha_aA_o}{\alpha_sA_i + \alpha_aA_o}, \quad \gamma_{b1} = 1 - \gamma_{a1}$$

$$\tau_{a1} = \frac{A\rho_{12}L_{120+Bend}}{M_1}, \quad \tau_{w1} = \frac{C_m}{\alpha_sA_i + \alpha_aA_o}$$

$$\alpha_1 = \frac{\alpha_sA_i\alpha_aA_o}{\alpha_sA_i + \alpha_aA_o}\frac{L_{120}}{M_1c_{p12}}, \quad c_1 = \alpha_1\frac{\gamma_{b1}}{\gamma_{a1}}$$

$$\Theta = \Theta_0 + \theta, \quad \Theta_m = \Theta_{m0} + \theta_m$$

$$\Theta_{sa} = \Theta_{sa0} + \theta_{sa}, \quad M_1 = M_{10} = M_{90}$$

$$\alpha_a = \alpha_{a0}, \quad \alpha_s = \alpha_{s0}, \quad \alpha_1 = \alpha_{10}$$

$$\rho_{12} = \rho_{120} = (\rho_{10} + \rho_{20})/2, \quad c_1 = c_{10}$$

$$\gamma_{a1} = \gamma_{a10}, \quad \gamma_{b1} = \gamma_{b10}, \quad \tau_{a1} = \tau_{a10}$$

The linearized equations of subcooled-liquid regions are given by:

$$\frac{\partial \theta}{\partial \ell} + \tau_{a20}\frac{\partial \theta}{\partial t} + \frac{\alpha_{20}}{\tau_{a20}}\theta = \frac{\alpha_{20}}{\gamma_{a20}}\theta_m \quad (29)$$

$$\tau_{a20}\frac{\partial \theta}{\partial t} = -\frac{\partial \theta}{\partial \ell} + \alpha_{20}(\Theta_{La0} - \Theta_{80})e^{-\alpha_{20}\ell}\left[\frac{\Delta\alpha_2}{\alpha_{20}} - \frac{\Delta\gamma_{a2}}{\gamma_{a20}}\right] - \frac{\alpha_{20}}{\gamma_{a20}}(\theta - \theta_m) \quad (30)$$

$$\tau_{w20}\frac{\partial \theta_m}{\partial t} = \Delta\gamma_{a2}(\Theta_{La0} - \Theta_{80})e^{-\alpha_{20}\ell} + \gamma_{a20}\theta_{La} + \gamma_{b20}\theta - \theta_m \quad (31)$$

where

$$\gamma_{a2} = \frac{\alpha_aA_o}{\alpha_LA_i + \alpha_aA_o}, \quad \gamma_{b2} = 1 - \gamma_{a2}$$

$$\tau_{w2} = \frac{C_m}{\alpha_LA_i + \alpha_aA_o}$$

$$\tau_{a2} = \frac{A\rho_{89}L_{890+U-Bend}}{M_8}$$

$$\tau_{w20}\frac{\partial \theta_m}{\partial t} = \gamma_{a20}\theta_{La} + \gamma_{b20}\theta - \theta_m$$

where

$$\alpha_1 = \frac{\alpha_sA_i\alpha_aA_o}{\alpha_sA_i + \alpha_aA_o}\frac{L_{12}}{M_1c_{p12}}$$

$$\gamma_{a1} = \frac{\alpha_aA_o}{\alpha_sA_i + \alpha_aA_o}$$

$$\gamma_{a10} = \frac{\alpha_{a0}A_o}{\alpha_{s0}A_i + \alpha_{a0}A_o}$$

$$\gamma_{b1} = 1 - \gamma_{a1}\frac{\alpha_sA_i}{\alpha_sA_i + \alpha_aA_o}$$

$$c_1 = \alpha_1 \frac{\gamma_{bl}}{\gamma_{al}} = \frac{\alpha_s A_i}{\alpha_s A_i + \alpha_a A_o}$$

$$\tau_{wl} = \frac{C_m}{\alpha_s A_i + \alpha_a A_o}$$

$$\tau_{al} = \frac{A \rho_{\overline{12}} L_{12+Bend}}{M_l}$$

2.4 Transfer functions and block diagrams

The transfer functions of the dynamic analysis are obtained by the combination of the basic equation, linearization and Laplace transformation of equations.

The transfer functions of the superheated-vapor region are obtained in the response of refrigerant temperature θ_2 in boundary 2 with the refrigerant inlet temperature θ_1, the flowed in air temperature θ_a and air velocity v_a according to the changes of the refrigerant flow rate m_1 are given by:

$$\theta_2(s) = \theta_1(s) e^{-f_1(s)} + \frac{\alpha_{10}[1-e^{-f_1(s)}]}{(1+\tau_{wl0}s) f_1(s)} \theta_a(s) - \frac{\beta_{10}}{\gamma_{al0}} \frac{\alpha_{10}[1-e^{-f_1(s)}]}{(1+\tau_{wl0}s) f_1(s)} \Delta\alpha_a(s) \quad (32)$$

$$\theta_2(s) = -\mu\alpha_1(1-\eta_{10}) \frac{1-e^{-h_1(s)}}{h_1(s)+\alpha_{10}} \frac{1+(1-\mu_1 c_{10})\tau_{wl0}s}{(1+\tau_{wl0}s)} \frac{(\Theta_{10}-\Theta_{a0})}{M_{90}} m_1(s) \quad (33)$$

where

$$f_1(s) = \tau_{al0}s + \alpha_{10} + c_{10} \frac{\tau_{wl0}s}{(1+\tau_{wl0}s)}$$

$$h_1(s) = \tau_{al0}s + c_{10} \frac{\tau_{wl0}s}{(1+\tau_{wl0}s)}$$

In the same method, the derivation of the transfer functions of the condensation starting region are given by:

$$\frac{K_3}{(1-T_3s)} m_4(s) + K_3(1-T_3s)\left[\frac{(1-T_{3B}s)}{K_{3C}} - \frac{1}{K_{3A}}\left\{(1-T_{3C}s) - \frac{K_{3B}}{(1+T_{3A}s)}\right\}\right]\theta_2(s) - \frac{K_3}{(1-T_3s)}\left[\frac{(1+T_{3B}s)}{K_{3C}} + \frac{1}{K_{3A}}\{(1-T_{3C}s) - \frac{K_{3B}}{(1+T_{3A}s)}\}\right]\theta_5(s) = \ell_{24}(s) \quad (34)$$

where gain constants and time lag are given by:

$$K_3 = \frac{L_{240}}{M_{90}}, \quad K_{3A} = \frac{2(\Theta_{30}-H_{3m0})}{M_{90}}$$

$$K_{3B} = \frac{\alpha_{s0}A_i}{\alpha_{s0}A_i + \alpha_{a0}A_o}, \quad K_{3C} = \frac{\Theta_{20}-\Theta_{40}}{M_{90}}$$

$$T_3 = \frac{A[\rho_{30}(H_{20}-H_{30}) - \rho_{40}(H_{20}-H_{40})]}{K_{140}(\Theta_{30}-\Theta_{sa0})} - \frac{C_m(\Theta_{3m0}-\Theta_{shm40})}{K_{140}(\Theta_{30}-\Theta_{sa0})}$$

$$T_{3A} = \frac{C_m}{\alpha_{st0}A_i + \alpha_{a0}A_o}, \quad T_{3B} = \frac{A\rho_{30}L_{240}}{2M_{90}}$$

$$T_{3C} = \frac{A(H_{20}-H_{30})}{\alpha_{s0}A_i}\left[\left(\frac{\partial\rho_3}{\partial p_d}\right)_{\Theta_{3c}}\left(\frac{\partial p_d}{\partial\Theta_5}\right)_0 + \left(\frac{\partial\rho_3}{\partial\Theta_3}\right)_{P_d}\right]$$

$$T_{3D} = \left[\frac{AL_{460}(H_{20}-H_{40})}{M_{90}}\right]\left(\frac{\partial\overline{\rho}_5}{\partial\Theta_5}\right)_0$$

$$T_{3E} = \frac{AL_{240}(\rho_{70}-\rho_{40})}{M_{90}}$$

$$T_{3F} = \frac{AL_{240}(\rho_{70}-\overline{\rho}_{50})}{M_{90}}$$

The transfer functions of the two-phase region and the condensation ending region are given by:

$$\frac{K_5}{(1+T_5s)} m_6 + \frac{K_5}{(1+T_5s)}\left[\frac{1}{K_{5C}} - \frac{1}{K_{5D}} - \frac{1}{K_{5A}}\left\{(1-T_{5C}s) - \frac{K_{5B}}{(1+T_{5A}s)}\right\}\right]\theta_5 \quad (35)$$
$$\frac{T_{5B}s}{(1+T_5s)} \ell_{24}(s) = \ell_{46}(s)$$

$$\frac{K_7}{(1-T_7s)}m_9(s)+\frac{K_7(1-T_{7B}s)}{K_{7C}(1-T_7s)}\theta_5(s)$$
$$-\frac{K_7}{K_{7A}(1-T_7s)}\left\{1-\frac{K_{7B}}{(1+T_{7A}s)}\right\}\theta_5(s)$$
$$-\frac{K_7}{K_{7A}(1-T_7s)}\left\{1-\frac{K_{7B}}{(1+T_{7A}s)}\right\}\theta_8(s) \quad (36)$$
$$+\ell_{24}(s)+\ell_{46}(s)=\frac{K_7(1+T_{7B}s)}{K_{7C}(1-T_7s)}\theta_8(s)$$

where

$$K_5=\frac{L_{460}}{M_{90}},\quad K_{5A}=\frac{(\Theta_{50}-\Theta_{5m0})}{M_{90}}$$

$$K_{5B}=\frac{\alpha_{T0}A_i}{\alpha_{T0}A_i+\alpha_{Ta0}A_o},\quad K_{5C}=\frac{(H_{40}-H_{60})}{M_{90}\left(\frac{\partial H_4}{\partial \Theta_4}\right)_0}$$

$$K_{5D}=\frac{(H_{40}-H_{60})}{M_{90}\left(\frac{\partial H_6}{\partial \Theta_6}\right)_0}$$

$$T_5=\frac{A[\rho_{60}(H_{40}-H_{60})-(\overline{\rho}_{50}H_{40}-\overline{\rho_{50}H_{50}})]}{K_{460}(\Theta_{50}-\Theta_{Ta0})}$$
$$+\frac{C_m(\Theta_{5m0}-\Theta_{shm60})}{K_{460}(\Theta_{50}-\Theta_{Ta0})}$$

$$T_{5A}=\frac{C_m}{\alpha_{T0}A_i+\alpha_{Ta0}A_o}$$

$$T_{5B}=\frac{A\rho_{60}(H_{40}-H_{60})+C_m(\Theta_{shm40}-\Theta_{shm60})}{K_{460}(\Theta_{50}-\Theta_{Ta0})}$$

$$T_{5C}=\frac{A}{\alpha_{T0}A_i}\left[H_{40}\left(\frac{\partial\overline{\rho}_5}{\partial\Theta_5}\right)_0-\left(\frac{\partial\overline{\rho_5H_5}}{\partial\Theta_5}\right)_0\right]$$

$$T_{5D}=\frac{AL_{460}(\rho_{70}-\rho_{60})}{M_{90}}$$

$$K_7=\frac{L_{680}}{M_{90}},\qquad K_{7A}=\frac{2(\Theta_{70}-\Theta_{7m0})}{M_{90}},$$

$$K_{7B}=\frac{\alpha_{L0}A_i}{\alpha_{L0}A_i+\alpha_{La0}A_o}$$

$$K_{7C}=\frac{\Theta_{60}-\Theta_{80}}{M_{90}}$$

$$T_7=\frac{A\rho_{70}(H_{60}-H_{70})+C_m(\Theta_{shm60}-\Theta_{7m0})}{K_{690}(\Theta_{70}-\Theta_{La0})}$$

$$T_{7A}=\frac{C_m}{\alpha_{L0}A_i+\alpha_{La0}A_o},\quad T_{7B}=\frac{A\rho_{70}L_{680}}{2M_{90}}$$

The transfer functions of the subcooled-liquid regions are possible by using the same method for the superheated-vapor region.

$$\theta_9(s)=\mu_{a2}(1-\eta_{20})\frac{1-e^{-h2(s)}}{h_2(s)+\alpha_{20}}$$
$$\frac{1+(1-\mu_2C_{20})\tau_{w20}s}{(1+\tau_{w20}s)} \quad (37)$$
$$\frac{(\Theta_{La0}-\Theta_{80})}{M_{90}}m_8(s)$$

where

$$\eta_{20}=1-e^{-\alpha_{20}},\qquad \mu_{a2}=M_{80}\frac{\Delta\alpha_2}{\Delta M}$$

$$\mu_{\gamma 2}=\frac{M_{90}}{\gamma_{b20}}\frac{\Delta\gamma_{a2}}{\Delta M},\qquad \mu_2=\frac{\mu_{\gamma 2}}{\mu_{a2}}$$

The block diagram in each region was drawn for the transfer function. The whole block diagram among the variable disturbances can be described through the combination of the transfer functions in each region such as the superheated-vapor region, condensation starting region, the two-phase condensing region, condensation ending region, and subcooled-liquid region.

Figure 2 shows the dynamic characteristic block diagram of entire condenser combined each region. Transfer function of each region is the same as Table 1.

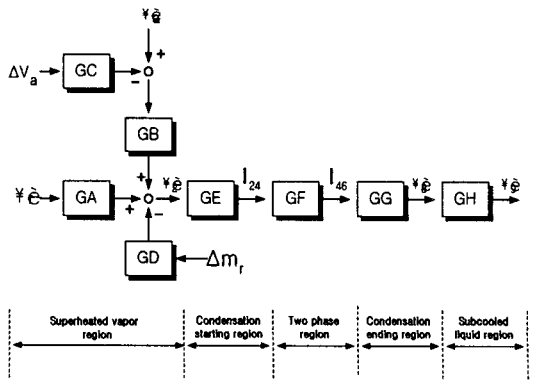

Fig. 2 Block diagram of air-cooled condenser.

Table 1 Transfer functions of the each region in air-cooled condenser

Symbols	Transfer functions
GA	$\mathrm{EXP}\left[-\left\{\alpha_{10}S+\tau_{a10}S+C_{10}\frac{\tau_{w10}S}{(1+\tau_{w10}S)}\right\}\right]$
GB	$\alpha_{10}\left(1-\mathrm{EXP}\left[-\left\{\alpha_{10}S+\tau_{a10}S+C_{10}\frac{\tau_{w10}S}{(1+\tau_{w10}S)}\right\}\right]\right) /(1+\tau_{w10}S)\left[\alpha_{10}+\tau_{a10}S+C_{10}\frac{\tau_{w10}S}{(1-\tau_{w10}S)}\right]$
GC	$\beta_1 \,/\, \gamma_{a1}$
GD	$\mathrm{EXP}(-\alpha_{10})(\theta_{10}-\theta_{sa1})\frac{\Delta\alpha_1}{\Delta M}$ $\frac{1-\mathrm{EXP}\left[-\left\{\tau_{a10}S+C_{10}\frac{\tau_{w10}S}{(1+\tau_{w10}S)}\right\}\right]}{\tau_{a10}S+C_{10}\frac{\tau_{w10}S}{(1+\tau_{w10}S)}}$
GE	$\frac{K_3}{(1-T_3S)}\left[\frac{(1-T_{3B}S)}{K_{3C}}-\frac{1}{K_{3A}}\left\{(1-T_{3C}S)-\frac{K_{3B}}{(1+T_{3A}S)}\right\}\right]\mathrm{EXP}(-\tau_{240}S)+\frac{1-T_3S}{1+(T_{3E}-T_3)S}$
GF	$\frac{1-T_{5B}S}{1+(T_5+T_{5D})S}\mathrm{EXP}(-\tau_{40}S)+\frac{1}{1+\frac{K_{7C}}{K_{7A}(1+T_{7B}S)}\left[1-\frac{K_{7B}}{(1+T_{7A}S)}\right]}$
GG	$\mathrm{EXP}\left[-\left\{\alpha_{20}+\tau_{a20}S+\frac{C_{20}\tau_{w20}S}{(1+\tau_{w20}S)}\right\}\right]$
GH	$\frac{K_{7C}(1-T_7S)}{K_7(1+T_{7B}S)}\mathrm{EXP}(-\tau_{680}S)$

3. Results and Discussion

3.1 Responses of each region

The dynamic characteristic of output values (θ_2, l_{24}, l_{46}, θ_8 and θ_9) which is related on each input values (Δv_a, Δm_r, θ_r and θ_a) are evaluated to gain and time constant by frequency response method at the board diagram. Here, the gain stands for output vibration rate for input and the time constant shows output time difference for input.

Table 2 shows feature and operating conditions of air-cooled condenser, Δv_a, Δm_r, θ_r and θ_a in Table 2 are the change quantity on the basis of steady-state value.

Table 2 Specifications and operating conditions

Items	Features		
Fin area	38.1mm × 231mm × 301ea (6.707ea/cm)		
Length of condensing tube	length of included bend : 12.978m		
Diameter	I. D. : 9.39mm, O. D. : 10.11mm		
Parameters	**Static conditions**	**Dynamic conditions**	**Ranges**
Condensing temperature, (℃)	49	49	constants
Condensing pressure, (kPa)	1955	1955	〃
Air velocity, (m/s)	1.09	0.89~1.29	Δv_a: ±0.2
Refrigerant flow rate, (kg/s)	0.0134	0.011 ~ 0.015	Δm_r: ±0.002
Refrigerant temperature, (℃)	98.0	97.0~99.0	$\Delta\theta_r$: ±1
Air temperature, (℃)	30	27~33	$\Delta\theta_a$: ±3
Refrigerant	HCFC-22		

Figure 3 shows the responses of refrigerant outlet temperature (θ_2) in the superheated-vapor region by the frequency response method. In the gain diagram of Fig. 3, the change of the flowed in air velocity showed a large gain value(45dB) in the low frequency band, but when moving toward the high-frequency band, its effect was small. But the influence of refrigerant inlet temperature increased when moving toward the high frequency band almost linearly. Also, the change of the refrigerant flow rate showed a constant tendency. With the input of the total disturbances, it showed the

highest gain around a frequency of 1×10^{-1} (rad/sec). In the phase diagram of Fig. 3, the flowed in air temperature and velocity showed a similar tendency; the refrigerant inlet temperature showed about 240 degrees of phase delay constantly. And with the input of the total disturbances, it showed a decreasing tendency when moving toward the high frequency band. Also, the flowed in air temperature and velocity showed a similar response in the superheated-vapor region, and the change of the refrigerant flow rate did not affect the refrigerant outlet temperature in the region. The reason is that the state of the refrigerant in this region hardly changes when various disturbances input; the average heat transfer coefficient on the refrigerant side barely changes and the gain and time delay constants are not affected.

Figure 4 shows the responses of length (l_{24}) in the condensation starting region. In the gain diagram of Fig. 4, the change of the refrigerant flow rate and the flowed in refrigerant temperature indicated a large influence when moving toward the high-frequency band and an almost similar response in characteristics. But the flowed in air velocity almost showed a second response characteristic; the flowed in air temperature showed a similar tendency with the air outlet temperature in the superheated vapor region. The total response was high from a frequency of 1×10^{-1} to 1×10^{1} (rad/sec). In the phase diagram of Fig. 4, the change of the refrigerant inlet temperature and the flowed in air velocity showed an almost similar response qualitatively; the flowed in air temperature and the refrigerant flow rate indicated a corresponding influence in the high-frequency band. The total response of the phase showed a decreasing tendency when moving toward a high frequency.

The reason is that the change of the refrigerant flow rate and flowed in temperature largely affect the heat transfer coefficient of the refrigerant; thus the gain and time constants

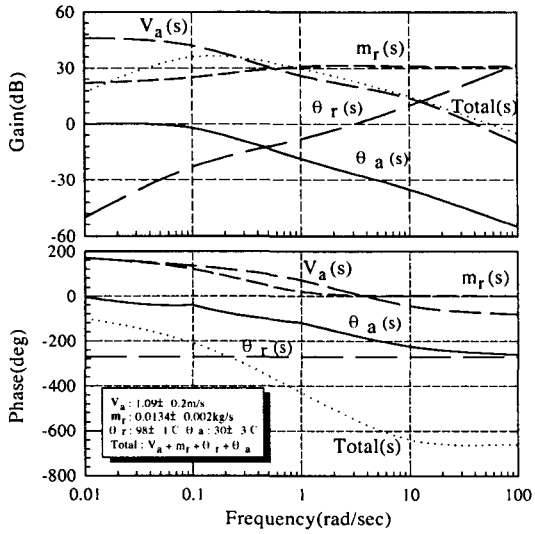

Fig. 3 Responses of outlet temperature (θ_2) in the superheated-vapor region.

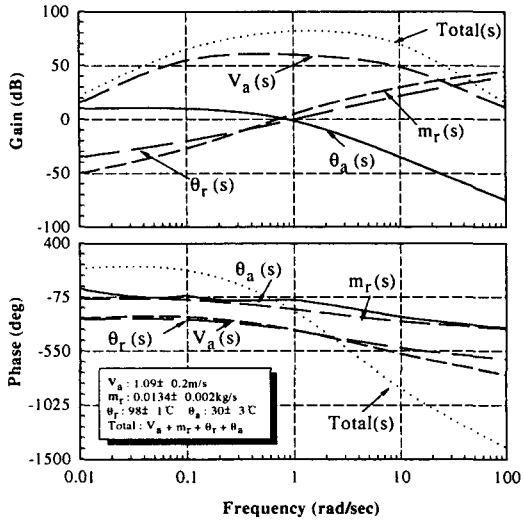

Fig. 4 Responses of length (l_{24}) in the condensation starting region.

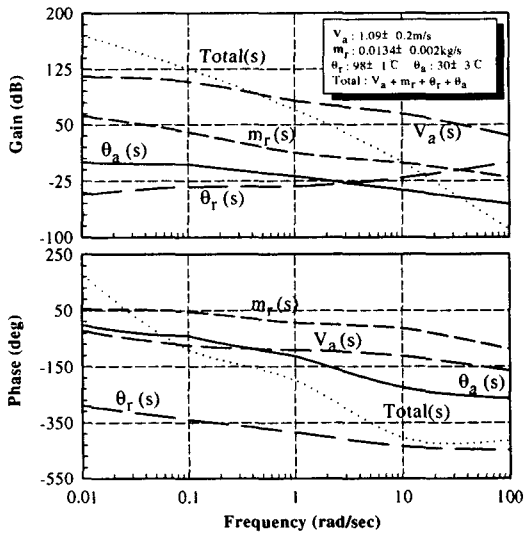

Fig. 5 Responses of length (l_{46}) in the two-phase condensing region.

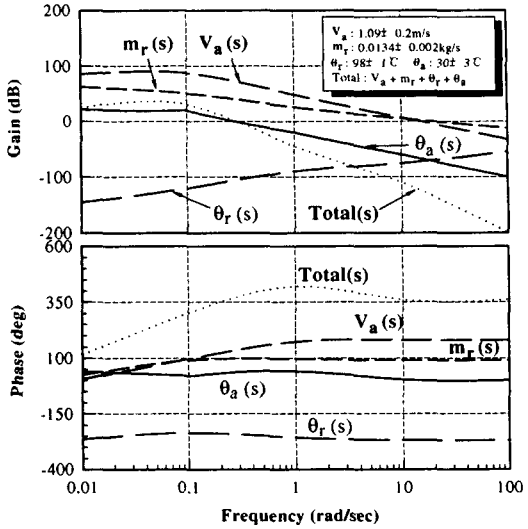

Fig. 6 Responses of outlet temperature (θ_8) in the condensation ending region.

affect the responses of length in this region.

Figure 5 shows the responses of length (l_{46}) in this region when the various disturbances input. In Fig. 5, the change of the flowed in air velocity showed the highest in the length of this region; the gain values of all disturbances were decreased when moving toward the high-frequency band, and the change in values showed low in the whole frequency range. But the phase delay in Fig. 5 was greatly influenced by the change of refrigerant temperature; the change of the refrigerant flow rate showed the fastest response.

The response of the total phase was described by a time delay response of high degree. The reason is that the responses of length in this region depend on the heat transfer coefficient on the air side.

Figure 6 shows the responses of outlet temperature (θ_8) in the condensation ending region when various disturbances input. In Fig. 6, the change of the flowed in air velocity indicated the largest influence in the low-frequency band, and the changes of the refrigerant flow rate and the flowed in air temperature showed a decreasing tendency in the high-frequency band, with the tendencies being very similar. But when the refrigerant temperature changed, it increased when moving toward the high-frequency band. In Fig. 6, the change of the flowed in air velocity showed a rapid-phase delay; other disturbances showed almost a constant phase delay, and the response of the total phase showed a response of nearly a secondary degree. The reason is that the outlet temperature in this region depends on the heat transfer coefficient on the air side in the low-frequency band, depends on the heat transfer coefficient on the refrigerant side in the high-frequency band.

Figure 7 shows the responses of outlet temperature in the subcooled-liquid region when the various disturbances input. In the gain diagram of Fig. 7, the change of the flowed in air veloc-

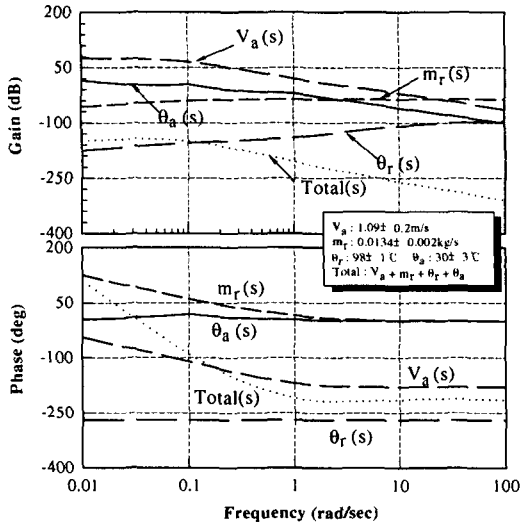

Fig. 7 Responses of outlet temperature (θ_9) in the subcooled-liquid region.

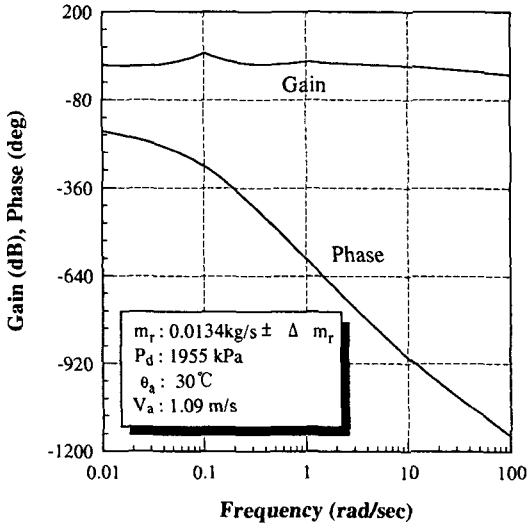

Fig. 8 Response of outlet temperature (θ_9) depending on the change of refrigerant flow rate.

ity indicated the highest influence in the low-frequency band. And the change of the refrigerant flow rate did not show any influence in the whole frequency range. But the change of the flowed in refrigerant temperature showed an increasing gain value when moving toward the high-frequency band. In the phase diagram of Fig. 7, the response of all disturbances showed a constant tendency after a frequency of 1×10^0(rad/sec). The reason is that heat transfer coefficients on the refrigerant and air side change; thus gain, time and time delay constants affect the responses of the outlet temperature.

3.2 Responses of the total region

From the results of the dynamic analysis in each region, the dynamic responses of outlet temperature in the condenser were analyzed by combining the transfer functions of each region in the block diagram when various disturbances are operating in the condenser.

Figure 8 shows the response of outlet temperature (θ_9) in the condenser when the change of the refrigerant flow rate is operating in the total region of the condenser. In the figure, the gain value indicated almost no influence in the total frequency range, but the phase delay showed high in the high-frequency range. These results revealed differences from that of Fig. 7 in only the subcooled-liquid region. It is believed that the time delay and time constants were affected by the heat capacity of the tube wall, the heat transfer coefficients on the refrigerant and tube-wall side.

Figure 9 shows the response of outlet temperature (θ_9) when the change of the air velocity operates in the total region simultaneously. In the figure, the gain and phase values decreased when moving toward the high-frequency range. These results showed differences from that of Fig. 8.

Figure 10 shows the response of outlet

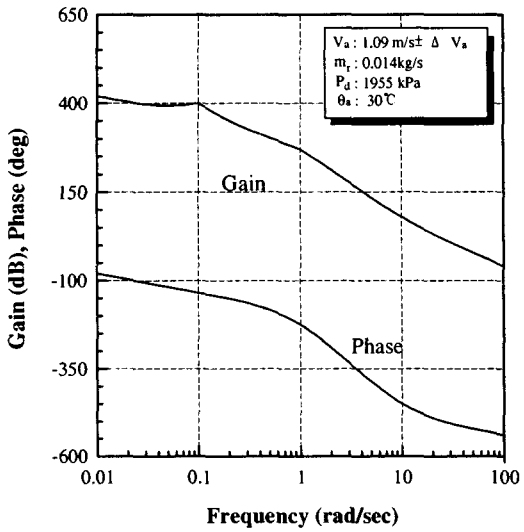

Fig. 9 Response of outlet temperature (θ_9) depending on the change of air velocity.

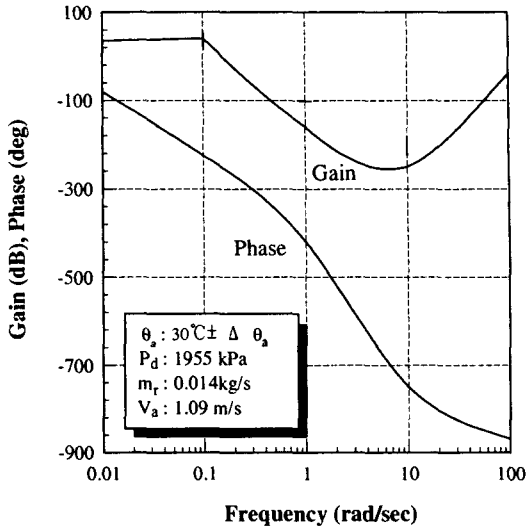

Fig. 10 Response of outlet temperature (θ_9) depending on the change of air temperature.

temperature (θ_9) when the change of the air temperature is operating in the total regions simultaneously. Figure 11 shows the response of the condenser outlet temperature (θ_9) in the condenser when disturbances, such as the change of the refrigerant flow rate, the air velocity, the air and refrigerant temperature operate simultaneously. In the figure, the responses of gain and phase showed response characteristics of a high degree. Also, these results showed differences from those of Figs. 8~10 quantitatively and qualitatively. It is believed that the gain, time constant, and time delay were a little different. Also, these were affected by the heat transfer coefficient on the refrigerant and air side.

4. Conclusions

The transfer functions for the dynamic characteristics in the condenser were obtained from the basic equations by linearizations and Laplace transformations of equations when various disturbances, such as the refrigerant flow rate, refrigerant temperature, air velocity, and air temperature inputted. The analyses of the dynamic characteristics were performed by the frequency response method, and the results of this study can be described as follows:

The development of a block diagram on the dynamic characteristics analysis in the condenser makes possible by linearizations of the basic equations, the derivation of transfer functions, and combination of these when various disturbances input. Effects of various disturbances on the actual condensers were analyzed by the frequency-response method, and the basic design data in the condenser were obtained quantitatively and qualitatively. Sufficient data were obtained to analyze the dynamic characteristics in the total system on the basis of these results. Therefore, these results may be used for the determination of design param-

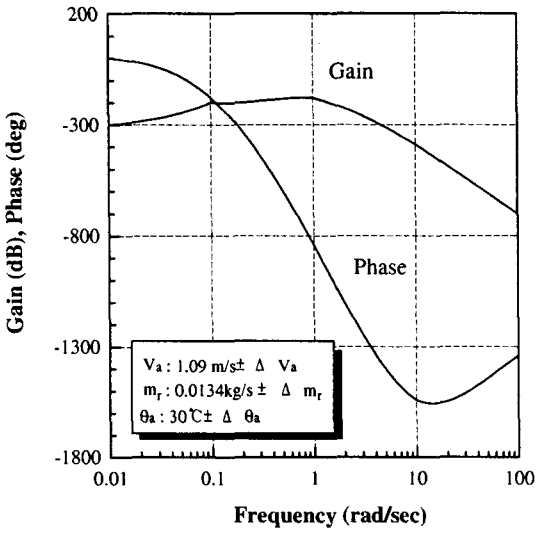

Fig. 11 Response of the condenser outlet temperature (θ_9) in the condenser when the disturbances operate simultaneously.

eters in actual components and entire systems. Also, the mathematical models, frequency response and steady-state response may be used to increase understanding, obtain useful information at the evaluation hardware and optimum design parameters, design control systems and determine the best controller settings for the refrigeration and air-conditioning systems. Moreover, the dynamic response characteristics may be clear from each calculation result of these responses and may be useful for a suitable design and the improvement of the control systems of refrigeration and air-conditioning systems.

Acknowledgment

The authors wishes to acknowledge the financial support of the Korea Research Foundation made in the program year of 1997

References

(1) Higuchi, K., 1986, "Evaporator Control systems", *Refrigeration*, Vol. 61, No. 701, pp. 1-8.

(2) Yasuda, H., 1992, "Development of Refrigeration Cycle Model by Transfer Function Method", *Proceedings of 1992 JAR Annual Conference*, pp. 101-104.

(3) Hamilton, J. F., Miller, J. L., 1990, "A Simulation Program for Modeling an Air-Conditioning System", *ASHRAE Trans.*, Vol. 96, Part 1, pp. 213-221.

(4) Ono, T., Sun, J., 1993, "On the Method of Linear System Identification Considering the Dynamics of Measuring Devices", *Trans. of the Society of Instrument and Control Engineers*, Vol. 29, No. 10, pp. 1141-1146.

(5) Kim, J. D., Yoon, J. I., Ku, H. G., 1997, "Dynamic Analysis of Evaporator Characteristics", *KSME International Journal*, Vol. 11, No. 2, pp. 221-228.

(6) James, R. W., 1986, "Dynamic Analysis of Refrigeration Systems", *Australian Refrigeration Air Conditioning and Heating*, pp. 31-38.

(7) Matsuoka, F., 1989, "Refrigeration Cycle of Transient Refrigerant Distribution", *Proceedings of the 23th Japanese Joint Conference on Air-conditioning and Refrigeration*, pp. 29-32.

(8) Nozu, S., 1982, "Calculation Method for the Tube Length and Pressure Drop of Air-Cooled Condensers", *Refrigeration*, Vol. 57, No. 660, pp. 41-53.

(9) Nozu, S., 1983, "Expressions for Mean Condensing Heat Transfer Coefficient and Friction Factor for Air-Cooled Condensers", *Refrigeration*, Vol. 58, No. 627, pp. 1-9.

(10) Yoshikawa, T., 1993, "Inverter for Refrigerator and Air Conditioner", *Refrigeration*, Vol. 68, No. 791, pp. 57-62.

(11) Kim, J. D., Oh, H. K., Yoon, J. I., 1995, "A Study on Dynamic Characteristics of a Refrigeration System by Controlling the Evaporator Superheat", *Transactions of Korean Society of Mechanical Engineers*, Vol. 19, No. 8, pp. 2012-2021.

(12) Kim, J. D., Oh, H. K., Yoon, J. I., Ku, H. G., 1996, "A Study on Optimal Control of Multi-Air Conditioning System", *Proceedings of the KSME 1996 Spring Annual Meeting Part-A*, pp. 279-282.

(13) Yamamoto, T., 1983, "Capacity Proportional Control Room Air Conditioner by instituted Toshiba Inverter", *Refrigeration and Air Conditioning Technology*, Vol. 34, No. 404, pp. 13-20.

(14) Higuchi, K., Hayano, M., 1982, "Dynamic Characteristics of Thermostatic Expansion Valve", *International Journal of Refrigeration*, Vol. 5, No. 4, pp. 216-220.

(15) Farzad, M., Oneal, D. L., 1991, "System Performance Characteristics of an Air Conditioner over a Range of Charging Conditions", *International Journal of Refrigeration*, Vol. 14, pp. 321-328.